Hindawi
Wireless Communications and Mobile Computing
Volume 2023, Article ID 3770982, 8 pages
https://doi.org/10.1155/2023/3770982

Research Article

Edge UAV Detection Based on Cyclic Spectral Feature: An Intelligent Scheme

Zhanbin Zhang,[1] **Wenjiang Ouyang**,[2] **Haitao Gao**,[2] **and Xiaojun Jing**[2]

[1]*School of Economics and Management, University of Chinese Academy of Sciences, Beijing, China*
[2]*School of Information and Communication Engineering, Beijing University of Posts and Telecommunications, Beijing, China*

Correspondence should be addressed to Zhanbin Zhang; zhangzhanbin17@mails.ucas.ac.cn

Received 20 September 2022; Revised 1 November 2022; Accepted 15 November 2022; Published 4 May 2023

Academic Editor: Peiying Zhang

With the commercialization of the fifth-generation mobile communication network (5G), the scale of the unmanned aerial vehicle (UAV) industry has continued to expand. However, the unregistered UAV has caused frequent harassment incidents at international airports, and the problem of UAV crimes is increasing. Radio technology supports long-distance detection of unregistered UAV and can be used as an efficient early warning method for unregistered UAV, which has attracted extensive attention from academia and industry. The classic UAV detection based on remote control signal method faces technical bottlenecks such as being easily affected by environmental noise, high complexity, and low detection accuracy. In the paper, an UAV remote control signal detection method is proposed based on cyclic spectrum features. More specifically, a dataset of UAV remote control signal UAV-CYCset is firstly constructed in the frequency domain. Based on UAV-CYCset dataset, a network architecture is proposed based on improved AlexNet, and the average detection accuracy of the improved model reaches 85% (from -10 dB to 10 dB) according to the simulation experiments.

1. Introduction

In recent years, unmanned aerial vehicle (UAV) has developed rapidly in civilian and has been widely used in aerial photography, agriculture, plant protection, disaster relief, transportation, surveying and mapping, remote sensing, and communications. With the continuous development of UAV, the scale of the industry is also increasing gradually, the fields of application have also been greatly expanded, and the market coverage is increasing year by year. At the same time, with the application of the fifth-generation mobile communication network (5G) in business [1], the data transmission range is wider, the stability is higher, and the delay is smaller. It contributes to the continuous expansion of the application scenarios of UAV and the rapid development of UAV under the impetus [2–4]. With the rapid rise of the UAV industry, many problems have also arisen. Reports of UAV endangering the lives of the public, violating the privacy of others, delaying flights, etc. are not uncommon. As a result, UAV detection has attracted more and more attention in industry and academia.

UAV is widely applied to different fields and is used by the public as one of the means of daily entertainment. It also affects people's normal life to a certain extent and even threatens national security. Most countries have begun to formulate policies to restrict the flight of UAV, the research on related technical means of UAV detection and interference is increased, and the control measures for UAV safety incidents are strengthened.

The main way to monitor and counter UAV is signal detection. The existing detection technologies mainly include (1) radar technology: the radar used in the anti-UAV solution uses one of the following three technologies: pulse (with source), CW (active), and CW (passive) modes. Each method has different characteristics and advantages and disadvantages [5, 6]. (2) Photoelectric technology: use optical cameras to capture scene images, and use infrared imaging or visible light technology to identify targets, to

achieve the purpose of tracking and positioning UAV [7, 8]. (3) Sound wave recognition: this technology will store the sound sample data of the UAV in the system in advance, collect the sound data in the environment during the monitoring process, and compare it with the sample data, finally determining the present state of the UAV. In the process of research on UAV flight, some researchers select the feature vector of sound spectrum, including voiceprint energy, MFC.C feature vector, and use support vector machine (SVM) to detect whether the UAV signal exists. In the actual application process, especially for environments with many residents or relatively noisy environments such as games, the method of sound wave identification will be seriously affected, and the detection distance will also be limited. (4) Radio technology: determine whether there is an UAV by detecting whether there is an UAV remote control signal or image transmission signal in the target area [9].

At present, UAV is becoming smaller and lighter, so the radar detection technology is getting more and more difficult to detect civilian UAV. Similarly, optoelectronic technology has high hardware requirements, and an UAV that is tens of meters away may only have a few pixels on the image, making identification difficult. At the same time, the harsh weather environment also causes many difficulties for optoelectronic technology. At present, with the development of technology, the wireless domain signal detection technology has become mature. Based on the electromagnetic signal detection technology combined with the wireless signal detection technology, the research on the technology suitable for detecting the remote-control signal of the UAV is also the current solution to the detection of the cooperation and noncooperation UAV in the complex environment, which is also the core of this paper.

1.1. Related Work. The current UAV detection and identification technology are still based on radar, optoelectronic technology, and wireless signals to detect UAV.

The research and development team of the University of California, San Diego, has built a 5G communication Frequency Modulated Continuous Wave (FMCW) long-distance high-resolution radar system based on 28 GHz phased array in terms of radar detection of UAV signals and detected targets up to 250 meters away with a resolution of 0.15 meters at distance. Ezuma et al. [10] of North Carolina State University in the United States detected and identified UAV through the RF fingerprint of the signal sent by the controller to the micro-UAV and used the energy transient signal to classify the UAV, using the k-nearest neighbor method. For UAV target detection, the average detection accuracy rate is 96.3%. The team from Nanyang Technological University in Singapore [11] designed a low, slow, and small radar target recognition method such as UAV and proposed a two-dimensional regularized complex logarithmic Fourier transform, which better solves the existing signal representation problem. At the same time, the literature proposes a subspace reliability analysis method to optimize the unreliable feature dimension of the conditional covariance matrix. In [12], Yang et al. used spectrum accumulation (SA) and statistical fingerprint analysis (SFA) techniques to estimate the frequency of UAV RF signals and then determine whether there is an UAV in the detection environment. The recognition rate of this method is close to 100% in the range of 2.4 km, and the recognition rate is greater than 90% in the range of 3 km. [13] proposed a radar-assisted positioning method based on 5G millimeter wave, deployed 5G millimeter wave radar, obtained additional features with the help of micro-Doppler characteristics, and then judged and identified the UAV rotor. On this basis, the sine frequency modulation (SFM) parameter optimization method is used to separate multiple UAV and realize the simultaneous detection of multiple UAV under the same conditions. Zhao and Su [14] from the National University of Defense Technology proposed a weak Doppler (m-D) signal evaluation method for UAV based on cyclostationary phase analysis (CPA) and realized the effective detection of small UAV based on radar.

From the mid-to-late 1980s, some related scholars began to explore the cyclostationary characteristics of signals. At first, the first-order statistics and second-order statistics of signals were used to extract signal characteristics [15, 16]. With the continuous evolution of wireless communication technology, Gardner et al. mentioned spectral redundancy and related concepts for the first time, which greatly promoted the research progress related to second-order cyclic statistics. At the end of the 20th century, related scholars successfully applied high-order cycle statistics to practical engineering. For example, the detection and analysis of high-order cycle statistics helped to monitor the failure state of mechanical devices [17]. At present, signal detection methods based on cyclostationary features have attracted extensive attention. Wang et al. proposed a blind detection algorithm for frequency hopping signals based on cyclostationary characteristics, extended the asymptotically optimal χ^2 test method to the detection problem of frequency hopping signals, designed the relevant detection statistics, and completed the Gaussian white noise environment frequency hopping signal detection. The algorithm performs well above -2 dB, the detection probability is 100%, the detection performance drops sharply from -2 dB to -8 dB, and the detection probability is 0% when the signal-to-noise ratio is less than -8 dB [18]. Zhang et al. proposed a neural network spectrum sensing algorithm based on the cyclostationary feature of the signal. By calculating the cyclic autocorrelation function of the signal, perform plane slicing to generate images and label them to generate datasets [19]. The dataset is fed into an artificial neural network with eight hidden layers for training. The experimental results show that the model has good detection performance for the existence of BPSK signal and OFDM signal and still has a detection probability of more than 90% in the case of -20 dB. The algorithm mainly recognizes two kinds of fixed-frequency signals, BPSK and OFDM. Lu et al. proposed an UAV signal identification method based on the contour map of the frequency hopping signal. By performing a short-time Fourier transform on the signal, the contour features of the signal are extracted to construct a three-dimensional matrix and

then processed to generate data. The constructed dataset is fed into a convolutional neural network for training [20]. The final model has better recognition accuracy on the dataset, with a detection probability of up to 100% above -10 dB and a detection probability of about 75% at -15 dB. The image acquisition and processing process of the algorithm are relatively complicated, and it is necessary to calculate the maximum value at each time point and then adjust the threshold to obtain the signal contour. After that, the image is processed with contrast and grayscale, so that the entire model consumes a long time.

In practical applications, UAV remote control signals are not only affected by environmental noise but also interfered with by other fixed-frequency communication signals. Therefore, the performance of the proposed UAV signal recognition model based on time-domain image perception is limited by the fixed frequency signal interference problem. The cyclostationary characteristics of wireless signals have the advantage of being insensitive to environmental interference.

1.2. Motivation and Main Contribution. Motivated by mentioned above, to reduce the complexity of the model as much as possible, ensure the recognition performance of the algorithm at low signal-to-noise ratio, and improve the anti-interference ability of the algorithm for fixed-frequency signals during frequency hopping signal detection, this paper proposes a cyclic spectrum-based method. The main contributions are concluded as follows:

(1) A novel UAV-CYCset cyclic spectrum dataset with a signal-to-noise ratio ranging from -10 dB to 10 dB is constructed

(2) A network architecture is proposed based on improved AlexNet

(3) An UAV remote control signal detection method is proposed based on cyclic spectrum features, and the constructed dataset is trained and tested through improved AlexNet

2. System Model

2.1. Cyclostationary Signal. According to the definition, a cyclostationary signal is a nonstationary signal, but it has its own cycle. Usually, there is a lot of information in the cycle when the relevant statistics of the cyclostationary signal change. This paper focuses on its second-order cyclostationary characteristics to illustrate.

Assuming that $x(t)$ is a nonstationary signal and has zero mean, it becomes $x(t)x^*(t-\tau)$ after secondary transformation. The following is the time-varying correlation function expression for $x(t)$:

$$R_x(t,\tau) = E\{x(t)x^*(t-\tau)\}. \tag{1}$$

Assuming that the period of $x(t)x^*(t-\tau)$ is T_0, then taking the relevant theory of Fourier series as a reference, the sample collection of $x(t)x^*(t-\tau)$ with the period of T_0 is performed, so the following can be obtained. Statement expression:

$$\begin{aligned} R_x^{\infty}(t,\tau) &= E\{x(t)x^*(t-\tau)\} \\ &= \lim \frac{1}{2N+1} \sum_{n=-N}^{N} x(t+nT_0)x^*(t+nT_0-\tau). \end{aligned} \tag{2}$$

Since $R_x(t,\tau)$ takes T_0 as the period, the relevant function can be expanded through the Fourier series, and the function expansion is as follows:

$$R_x^{\infty} = \sum_{m=-\infty}^{\infty} R_x^{\infty}(t,\tau)e^{-j2\pi\alpha t}. \tag{3}$$

In the above formula, $\alpha = m/T_0$, and its Fourier series is

$$R_x^{\infty}(\tau) = \frac{1}{T_0}\int_{-T_0/2}^{T_0/2} R_x(t;\tau)e^{-j2\pi\alpha t}dt. \tag{4}$$

Bring equation (2) into equation (4) to get:

$$R_x^{\infty}(\tau) = \lim_{T\longrightarrow\infty} \frac{1}{T}\int_{-T/2}^{T/2} x(t)x^*(t-\tau)e^{-j2\pi\alpha t}dt. \tag{5}$$

The above formula expresses the time average of the correlation function. The coefficient $R_x^{\infty}(\tau)$ represents the degree of cyclic autocorrelation of the signal at frequency α, also known as the cyclic autocorrelation function. The value that obtains a nonzero value of $R_x^{\infty}(\tau)$ is called the cyclic frequency of the signal. This parameter mainly reflects the cyclostationary characteristics of the signal. Usually, there may be different cyclic frequencies in the corresponding specific signal.

If $\alpha = 0$, we have

$$R_x^0(\tau) = x\left(t+\frac{\tau}{2}\right)x^*\left(t-\frac{\tau}{2}\right)_t. \tag{6}$$

At this time, after $R_x^{\infty}(\tau)$ is degraded, it becomes the autocorrelation function of the stationary signal. If the signal satisfies $R_x^{\infty}(\tau) = 0, \forall \propto \neq 0$, it can be regarded as a stationary signal; and if it satisfies $R_x^{\infty}(\tau) \neq 0, \exists \propto \neq 0$, it belongs to a cyclostationary signal.

Cyclostationary signal itself does not have statistical characteristics. After a series of calculations, it can be found that some of its mathematical characteristics are periodic. The mathematical expectation in the first-order statistics of the cyclostationary signal and the signal autocorrelation function in the second-order statistics have been verified to be periodic. Therefore, it is possible to find and select an appropriate way to process the signal and convert the signal characteristics, which is beneficial to find the characteristics of the signal in essence. And whether it is first-order or second-order cyclostationary, its characteristics are related to the frequency shift signal, which mainly depends on the way of operation.

Because the cyclostationary signal processes the signal features in a corresponding way and completes the feature extraction, the processing of such signals is obviously different from the traditional signal processing methods. First of all, when processing cyclostationary signals, the signal characteristics obtained by transformation are the main components. Compared with directly processing the original signal, the processing of the cyclostationary signal will extract the simplified signal characteristics of the original signal, which will obviously reduce the complexity. Second, when analyzing the cyclostationary signal, the target is statistical information, which can reduce the interference caused by the noise with stationary characteristics and improve the anti-noise ability. Third, when dealing with actual signals, choosing cyclostationary signals for processing is more in line with reality, which not only ensures the rationality of the results but also makes the processing process easier. It is also because of the characteristics of the cyclostationary signal itself that the use of cyclostationary detection to receive signals has become the most widely used method. Cyclostationary detection is mainly used in the signal processing process to judge whether the signal has cyclostationary characteristics; second, if it is known that the signal has cyclostationary characteristics, even on the premise that the signal has cyclostationary frequency characteristics, this method is usually used to judge whether there is a known signal in the signal. The above applications make the cyclostationarity detection method more and more common in the current signal processing process.

2.2. Cycle Spectrum. The realization of the cyclic spectrum is mainly based on the digital fast Fourier transform. Common cyclic spectrum implementation algorithms mainly include three categories. The first is the time domain smooth estimation algorithm, and the formula is as follows:

$$S_x^{\infty}(t,f) = \frac{1}{\mathrm{KM}} \sum_{u=0}^{\mathrm{KM}-1} \Delta f X_{1/\Delta f}\left(t - \frac{u}{k\Delta f}, f + \frac{\alpha}{2}\right) X_{1/\Delta f} \cdot \left(t - \frac{u}{k\Delta f}, f + \frac{\alpha}{2}\right), \tag{7}$$

In the above formula, $X_{1/\Delta f}(t,f)$ represents the smooth DFT transform output; $\Delta f = 1/(N-1)T_S$ represents the spectral resolution. $1/\Delta f$ represents the length of the segment.

The second is the frequency domain smoothing estimation method, and the formula is as follows:

$$S_x^{\infty}(t,f)_{\Delta f} = \frac{1}{M} \sum_{v=-M-1/2}^{M-1/2} \frac{1}{\Delta t} X_{\Delta t}\left(t, f + \frac{\alpha}{2} + vF_S\right) X_{\Delta t}^{*} \cdot \left(t, f - \frac{\alpha}{2} + vF_S\right), \tag{8}$$

where $X_{\Delta t}(t,f)$ represents the output after sliding DFT operation. T_S represents the time sampling increment; $\Delta f = MF_S$ represents the spectral smoothing gap width; the total number of samples in the data segment of the time interval Δt is $N = (\Delta t/T_S) + 1$.

To sum up, the process that the output obtained after demodulation is processed by conjugate multiplication is the operation process of the FFT accumulation algorithm, so the computing power of the computer is relatively high when performing the two-dimensional fast Fourier transform operation, which usually requires more memory and takes more time to complete. The instantaneous correlation function algorithm first requires the calculation of the autocorrelation function of the nonstationary signal, then completes the transformation in the time domain and frequency domain, and then estimates the cyclic spectrum.

2.3. The Generation of Dataset. The frequency hopping signal used in this experiment is also generated by the modeling tool in MATLAB. The center frequency of the frequency hopping signal is 2.4 GHz, the signal rate is 50 Kb/s, the number of bits per hop is 50, and the bandwidth of the frequency hopping signal is 9.8 MHz. After the frequency hopping signal is generated, it also needs to go through the Rayleigh channel model containing Gaussian white noise. In this experiment, after obtaining the noisy signal noise, it is necessary to calculate the cyclic autocorrelation function of the signal and then perform the FFT operation on the function to obtain the spectral correlation function of the signal. Based on the theoretical knowledge described in the previous chapter, the spectral correlation function obtained using correlation operation has noise, signal spectral correlation function, and cross-spectral correlation function. The cyclic spectrum is to expand the spectral correlation function of the obtained noisy signal on the α-axis and the f-axis, so that the cyclic spectrum can be obtained, where α is an integer multiple of the fundamental frequency of the signal, and f represents the frequency of the signal. The cyclic spectrum is a three-dimensional image, and the height of its vertical axis is normalized to determine whether there is a main signal. Since the image we put into the convolutional neural network is two-dimensional, the experiment needs to map the three-dimensional image on the two-dimensional plane to ensure that the characteristics of the cyclic spectrum can be preserved to the greatest extent in the two-dimensional plane. In this experiment, the $\alpha - f$ plane is used as the benchmark to map the vertical axis of the plane. The experiment uses color to represent the amplitude of the spectral function at this point, as shown in Figure 1 below. The darker the color, the higher the amplitude value. Shallower values represent lower amplitude values.

The computational complexity of the cyclic spectrum is high. In this experiment, 2048 sample points are intercepted from the received signal to calculate the total to obtain the cyclic spectrum of the signal. Since the convolutional neural network needs control samples, this experiment uses the same algorithm to generate the cyclic spectrum of noise when generating the cyclic spectrum of the noisy signal, as shown in Figure 2. The signal-to-noise ratio range of the frequency hopping signal collected in this experiment is also -10~10 dB, with 1 dB as an interval. 100 signal time domain images and noise time-domain images were collected under different signal-to-noise ratio conditions.

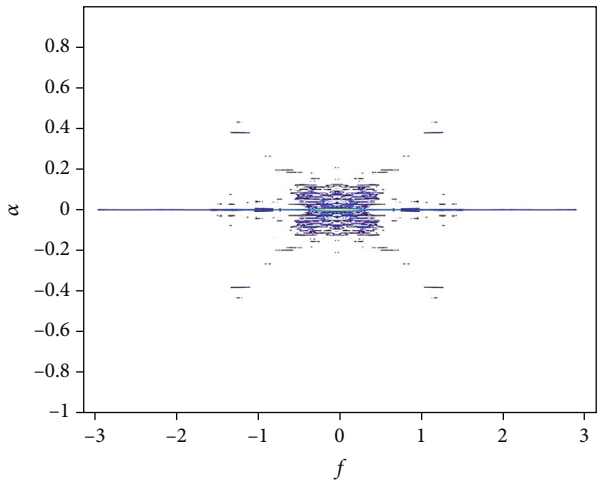

Figure 1: Frequency hopping signal cycle spectrum.

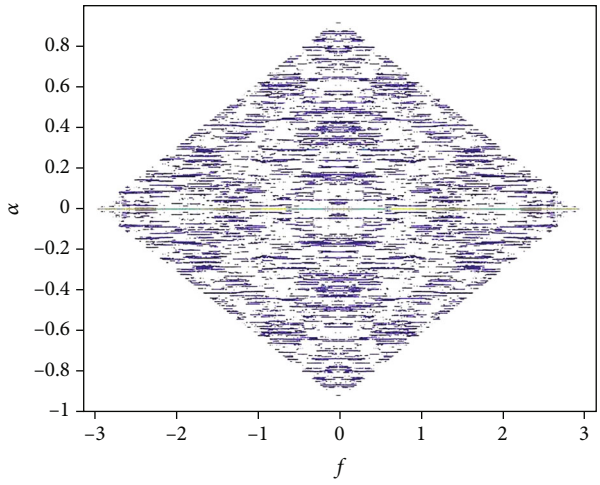

Figure 2: Noise cyclic spectrum.

After the acquisition of the image is completed, the pixels where the irrelevant information such as the horizontal and vertical coordinates in the input image are located are deleted, and only the cyclic spectrum image is retained. Then resize the image to 227*227*3, where 227 is the length and width of the image, and 3 is the number of channels of the image. After the image size processing is completed, the signal image and the noise image are labeled, respectively, and stored as record files. Each file includes the corresponding image and its corresponding label. The signal time domain image label is 1, and the noise image label is 0. Finally, generate the UAV-CYCset cyclic spectral dataset of UAV signals. In the experiment, 4200 time-domain images were obtained through MATLAB simulation, of which there were 100 signal and noise images under each signal-to-noise ratio. In this experiment, 70 signal images and 70 noise images under each signal-to-noise ratio are taken from UAV-CYCset, a total of 2960 images are used as the training set, and the remaining 1240 images are used as the test set.

3. Proposed Schemes

In the pretraining stage, this experiment considers a traditional convolutional neural network (CNN) for training. After the model converges, the expected effect is not achieved, and the recognition rate of the training set is lower than 85%. Considering that the cyclic spectrum of the signal has more feature points than the time domain image, and the size of the generated image is larger, the CNN network may not meet the experimental requirements of this experiment. After investigation and multiple pretraining experiments, the AlexNet model was selected as the basic experimental model in this experiment.

3.1. Model Architecture and Improvements. Under the premise of ensuring the recognition performance of the model, AlexNet [21] has fewer convolution layers, which reduces the complexity and time consumption of the model, and the input is 228*228, which reduces the impact on the recognition performance caused by the clipping and scaling of the circular spectrum image. The model has a total of eight hidden layers, of which the first five are convolutional layers, and the rest are fully connected layers. Among all convolutional layers, only layers 1, 2, and 5 use pooling operations. The improved AlexNet architecture is shown in Figure 3, and the parameters of AlexNet network are listed in Table 1.

The input data of the first layer is the image with the original size of 227*227*3, where 227 represents the image size, 3 represents the number of channels of the image, the convolution kernel size of this layer is 11*11, and the number of channels is the same as the number of image channels. The pixel layer output by the first layer is used as the input data of the second layer, the size of the pixel layer is 27*27*48, the pixel layer output by the second layer is used as the input data of the third layer, and the size of the pixel layer is 13*13*128. The pixel layer output by the third layer is used as the input data of the fourth layer. The size of the pixel layer is 13*13*192.

The fifth layer is the same as the fourth layer, and the output after the convolution operation is still 13*13*192. The sixth layer is a fully connected layer, which inputs data with a size of 6*6*256 and convolves the input data through filters of the same size. The 4096 data output in the seventh layer is fully connected to the 4096 neurons in this layer, and then the 4096 data formed by the activation function ReLU and Dropout operation are processed. The 4096 data input in the 8th layer is fully connected to the 1000 neurons in this layer, and the trained values are outputted externally after training.

This experiment has been optimized based on AlexNet. The ReLU function is used as the activation function in the AlexNet network model. The ReLU function can accelerate the convergence and solve the problem of gradient disappearance. However, because the negative semiaxis of the ReLU function is 0, the weight may not be updated because the derivative is 0. Therefore, in this experiment, the Swish activation function is used to replace the ReLU function. The Swish function formula is as follows:

$$f(x) = x\frac{1}{1+e^{-x}}. \tag{9}$$

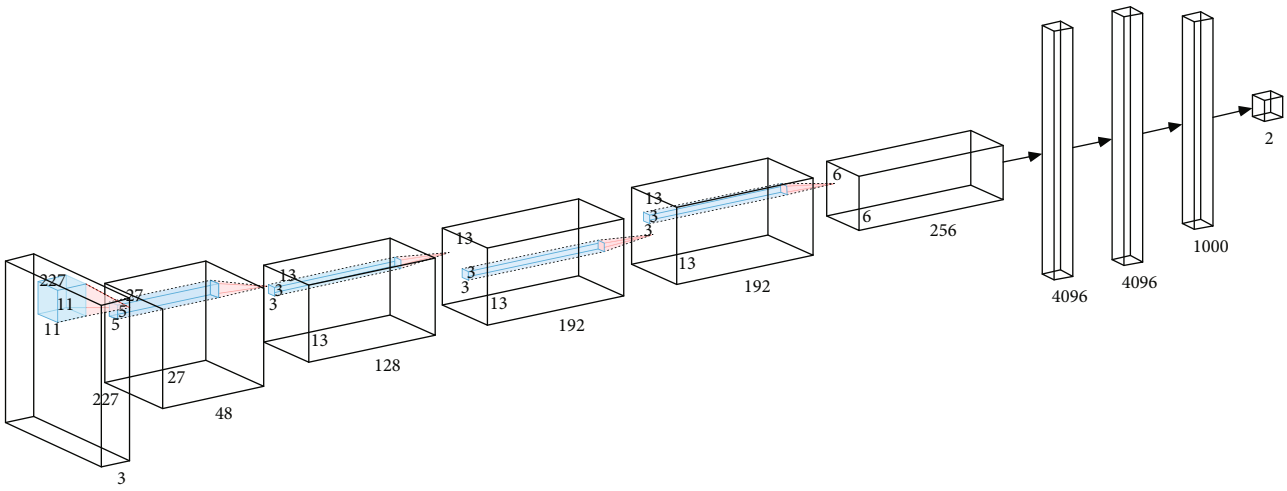

Figure 3: The architecture of the proposed improved AlexNet [21].

Table 1: The parameters of AlexNet network.

Model structure	Model parameter
Convolution layer1	48 (11×11)
MaxPool layer1	3×3
Convolution layer2	128 (5×5)
MaxPool layer2	3×3
Convolution layer3	192 (3×3)
Convolution layer4	192 (3×3)
Convolution layer5	256 (3×3)
MaxPool layer3	3×3
Fully connected layer1	4096
Fully connected layer2	4096
Fully connected layer3	1000
Fully connected layer4	2

Compared with the ReLU function, the Swish function does not have a derivative of 0. After pretraining and the comparison and verification of the ReLU function, the Swish function can better solve the problem that the weights caused by the ReLU function cannot be updated during the training process. At the same time, the Swish function also has a certain improvement in model overfitting. Since Adam requires fewer computing resources than RMSProp, this experiment chooses to use the Adam algorithm as the optimizer in model training.

3.2. Model Training. In the process of model training in this experiment, the signal sample images and noise sample images in the training set are scrambled, respectively, to generate sample queues. In each training, 50 samples are drawn from the team leaders in the two queues to form a small training set with a size of 100, and the small training set is sent to the neural network for training. After each training, the signal samples and noise samples in the small training set are put into the tail of their corresponding sample queues, respectively, and the previous operations are repeated to train the convolutional neural network.

In this experiment, a 10-fold crossover method is also used to test the accuracy of the algorithm. At the same time, 7 copies are selected as training data, and the rest are used as test data. The experiments are completed in turn, and the corresponding accuracy rate is obtained in each round. Take the average after 10 training runs, and the result is an estimate of the accuracy of the algorithm.

4. Simulation and Discussion

Since this experiment uses the self-built data set UAV-CYCset for training and testing, and there is no publicly related data set in the network, this experiment mainly compares the recognition performance of traditional algorithms. The comparison algorithm selected in this experiment is the blind detection algorithm of frequency hopping signal based on cyclic autocorrelation proposed by Fan Haining. The basic principle of the algorithm is to assume that the received signal is $x(n)$, the received signal contains the frequency hopping signal and noise, and the cyclic autocorrelation function is calculated for the received signal $x(n)$. The formula is as follows:

$$\widehat{R}_{xx}^{\alpha}(m) = \frac{1}{L}\sum_{n=0}^{L-1} x(n+m)x^{*}(n)\exp\left(-j2\pi\alpha n\right). \tag{10}$$

In the formula, L is the length of the received signal. After that, calculate the average power $\bar{P}_x$ of the received signal with the following formula:

$$\bar{P}_x = \frac{1}{L}\sum_{n=0}^{L-1} |x(n)|^2. \tag{11}$$

After that, a Gaussian white noise sequence $v(n)$ with the same length as the received signal is generated, the power of the Gaussian white noise is required to be equal to the

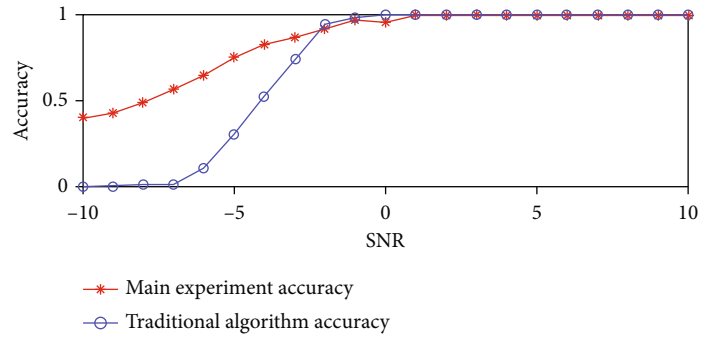

Figure 4: The comparison of accuracy between AlexNet and benchmark.

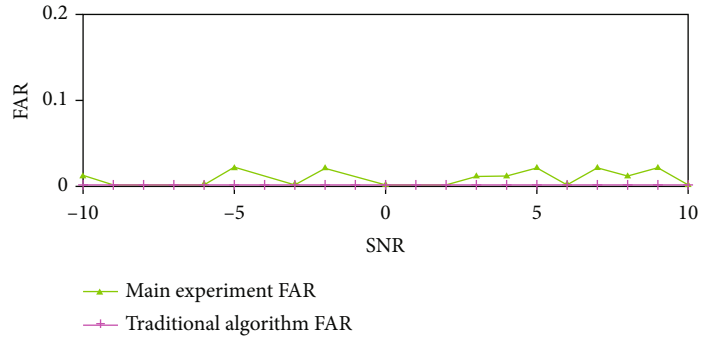

Figure 5: The comparison of false alarm rate between AlexNet and benchmark.

average power of the received signal, and then the cyclic autocorrelation function of $v(n)$ is calculated to estimate $\widehat{R}_w^{\alpha}(m)$. Select the maximum value of $\widehat{R}_w^{\alpha}(m)$ of $\max_{\alpha} \widehat{R}_w^{\alpha}(m)$ as the decision threshold th, artificially add a correction weight, set it as ω, and then whether the frequency hopping signal exists, the judging method is that if there is at least one α such that $|\widehat{R}_w^{\alpha}(m)| > th * \omega$, it is judged that there is a frequency hopping signal; otherwise, it is judged that there is only noise. The data length of the signal in this experiment is $L = 2048$, and the correction weight is 1.35.

In this experiment, the signal sample is a positive example. After the correlation operation, the recall rate of the convolutional neural network model can reach 85.05%, and the accuracy rate can reach 99.112%. It can be seen from the data that the convolutional neural network has a good recognition performance for the cyclic spectrogram of the UAV frequency hopping signal. The recall rate obtained by the comparison algorithm through experiments is 69.69%, and the precision rate is 100%. Since the sample contains signal and noise samples with different signal-to-noise ratios from -10 dB to 10 dB, the corresponding experiment results are exhibited as it is shown in Figures 4 and 5.

It can be seen from Figure 4 that the accuracy of the convolutional neural network in identifying signal samples has an upward trend. Although the recall rate of the convolutional neural network in the entire test set can reach 85.05%, the recognition rate of signal samples with low signal-to-noise ratio is poor. When the signal-to-noise ratio is lower than -5 dB, the probability of identifying the signal is less than 80%. If when the signal-to-noise ratio is -10 dB, the probability of identifying the signal is only 41%. Although the convolutional neural network model shows a downward trend as the signal-to-noise ratio decreases, this does not affect the excellent recognition performance of the neural network model in the case of high signal-to-noise ratio. If the signal-to-noise ratio exceeds 1 dB, the probability of identifying the signal can reach 100%. The counterexample sample in the experiment is the cyclic spectrogram of noise. As shown in Figure 5, the green line in the figure represents the false alarm rate of the main experiment, that is, the recognition rate of identifying the noise sample as a signal. The neural network performs well in the entire range of signal-to-noise ratio, the overall false alarm rate is only about 0.77%, and the signal-to-noise ratio change has no effect. The traditional algorithm has good recognition performance when the signal-to-noise ratio is greater than 0 dB, the signal recognition probability drops sharply between -2 dB and -7 dB, and the recognition rate is basically 0 when the signal-to-noise ratio is less than -7 dB.

Compared with the traditional algorithm, the model generated in this experiment has little difference in the case of high signal-to-noise ratio and performs well in the false alarm rate. As the signal-to-noise ratio decreases, the recognition rate of the network model will not drop drastically like traditional algorithms. At the same time, when the UAV is receiving the frequency hopping signal, it is possible to receive not only environmental noise but also signals

emitted by other transmitters. However, since most signals do not have cyclic characteristics, the cyclic spectrum is used as a convolutional neural network. The input of the model ensures the anti-interference performance of the neural network under the condition of other fixed-frequency signals to a certain extent and has great application value.

5. Conclusion

In this paper, a detection method of UAV remote control signal based on cyclic spectrum feature is proposed. First, the basic theory of the current cyclostationary theory is introduced, and the basic characteristics of the cyclostationary signal and the cyclic spectrum can be used as the theoretical basis for the detection of the frequency hopping signal. After that, the establishment of the cyclic spectral sample dataset is conducted. Based on the UAV-CYCset dataset of UAV remote control signal frequency domain, a network architecture is proposed based on improved AlexNet, and the average detection accuracy of the improved model reaches 85% (-10 dB-10 dB), which demonstrates the feasibility of using cyclic spectrogram as input to detect UAV frequency hopping signal using convolutional neural network.

Data Availability

The dataset is available. If need, contact the corresponding author.

Conflicts of Interest

The authors declare that they have no conflicts of interest.

References

[1] J. Mu, X. Jing, Y. Zhang, Y. Gong, R. Zhang, and F. Zhang, "Machine learning-based 5G RAN slicing for broadcasting services," *IEEE Transactions on Broadcasting*, vol. 68, no. 2, pp. 295–304, 2022.

[2] M. Mozaffari, W. Saad, M. Bennis, Y. Nam, and M. Debbah, "A tutorial on UAVs for wireless networks: applications, challenges, and open problems," *IEEE Communications. Survey*, vol. 21, no. 3, pp. 2334–2360, 2019.

[3] L. Gupta, R. Jain, and G. Vaszkun, "Survey of important issues in UAV communication networks," *IEEE Communication Surveys and Tutorials*, vol. 18, no. 2, pp. 1123–1152, 2016.

[4] J. Mu, F. Zhang, Y. Cui, J. Zhu, and X. Jing, "Non-cooperative UAV detection with adaptive sampling of remote signal," in *International Wireless Communications and Mobile Computing (IWCMC)*, pp. 791–795, Harbin City, China, 2021.

[5] N. Zhao, F. Cheng, F. R. Yu et al., "Caching UAV assisted secure transmission in hyper-dense networks based on interference alignment," *IEEE Transactions on Communications*, vol. 66, no. 5, pp. 2281–2294, 2018.

[6] C. Wang, J. Tian, J. Cao, and X. Wang, "Deep learning-based UAV detection in pulse-Doppler radar," *IEEE Transactions on Geoscience and Remote Sensing*, vol. 60, pp. 1–12, 2022.

[7] A. Rozantsev, V. Lepetit, and P. Fua, "Detecting flying objects using a single moving camera," *IEEE Transactions on Pattern Analysis and Machine Intelligence*, vol. 39, no. 5, pp. 879–892, 2017.

[8] Y. Bazi and F. Melgani, "Convolutional SVM networks for object detection in UAV imagery," *IEEE Transactions on Geoscience and Remote Sensing*, vol. 56, no. 6, pp. 3107–3118, 2018.

[9] X. Ai, L. Zhang, Y. Zheng, and F. Zhao, "Passive detection experiment of UAV based on 5G new radio signal," in *2021 Photonics & Electromagnetics Research Symposium (PIERS)*, pp. 2124–2129, Hangzhou, China, 2021.

[10] M. Ezuma, F. Erden, C. K. Anjinappa, O. Ozdemir, and I. Guvenc, "Micro-UAV detection and classification from RF fingerprints using machine learning techniques," in *2019 IEEE Aerospace Conference*, Big Sky, MT, USA, 2019.

[11] J. Ren and X. Jiang, "Regularized 2-D complex-log spectral analysis and subspace reliability analysis of micro-Doppler signature for UAV detection," *Pattern Recognition*, vol. 69, pp. 225–237, 2017.

[12] S. Yang, H. Qin, X. Liang, and T. Gulliver, "An improved unauthorized unmanned aerial vehicle detection algorithm using radiofrequency-based statistical fingerprint analysis," *Sensors*, vol. 19, no. 2, p. 274, 2019.

[13] J. Zhao, X. Fu, Z. Yang, and F. Xu, "Radar-assisted UAV detection and identification based on 5G in the internet of things," *Wireless Communications and Mobile Computing*, vol. 2019, Article ID 2850263, 12 pages, 2019.

[14] Y. Zhao and Y. Su, "Cyclostationary phase analysis on micro-Doppler parameters for radar-based small UAVs detection," *IEEE Transactions on Instrumentation and Measurement*, vol. 67, no. 9, pp. 2048–2057, 2018.

[15] A. Swami and B. M. Sadler, "Hierarchical digital modulation classification using cumulants," *IEEE Transactions on Communications*, vol. 48, no. 3, pp. 416–429, 2000.

[16] A. Abdelmutalab, K. Assaleh, and M. El-Tarhuni, "Automatic modulation classification based on high order cumulants and hierarchical polynomial classifiers," *Physical Communication*, vol. 21, pp. 10–18, 2016.

[17] L. Izzo and A. Napolitano, "Multirate processing of time series exhibiting higher order cyclostationarity," *IEEE Transactions on Signal Processing*, vol. 46, no. 2, pp. 429–439, 1998.

[18] M. Oner, "Spectral correlation of a digital pulse stream modulated by a cyclostationary sequence in the presence of timing jitter," *IEEE Transactions on Communications*, vol. 57, no. 2, pp. 339–342, 2009.

[19] L. Izzo, L. Paura, and G. Poggi, "An interference-tolerant algorithm for localization of cyclostationary-signal sources," *IEEE Transactions on Signal Processing*, vol. 40, no. 7, pp. 1682–1686, 1992.

[20] Y. Xie, P. Jiang, Y. Gu, and X. Xiao, "Dual-source detection and identification system based on UAV radio frequency signal," *IEEE Transactions on Instrumentation and Measurement*, vol. 70, pp. 1–15, 2021.

[21] T. Technicolor, I. Sutskever, and G. E. Hinton, "ImageNet classification with deep convolutional neural networks," *Communications of the ACM*, vol. 60, no. 6, pp. 84–90, 2017.